ISSN: 2994-6433

Research Article

Journal of Sensor Networks and Data Communications

Voronoi Structure of Space Integration with an Applied Roundabout Network - Part II

Ali Essam El-Shazly*

Department of Architectural Engineering, Fayoum University, Egypt

***Corresponding Author**
Ali Essam El-Shazly, Professor, Department of Architectural Engineering, Fayoum University, Egypt.

Submitted: 2024, Apr 19; **Accepted**: 2024, Jun 17; **Published**: 2024, Jul 08

Citation: El-Shazly, A. E. (2024). Voronoi Structure of Space Integration with an Applied Roundabout Network - Part II. *J Sen Net Data Comm, 4*(2), 01-11.

Abstract

The dual Delaunay graph of Voronoi network unfolds into various geometric and topological properties of intangible space structure. Specifically, objective space integration of Delaunay layout determines the parameters of universal distance, distributiveness, geometric moments and traversable properties with their correlation in a single graph network. The pilot application on the network of roundabout Cairo defines the original space integrity for future conservation. The resultant analysis satisfies the hamiltonian circuiting with the highest layout integration of generator-9 in correlative measurements. On the contrary, the least integral generator-13 maintains the close ties with the adjacent generator-14 of better layout connectivity in compensation. Nevertheless, the core generators 3 & 4 of the layout form a dense overlapping circumcircle in correlation to cyclic graph minors, which boosts the global system integration. Future overview on computational Delaunay-graph of programmable network properties amalgamates a robust integral structure of space in prospective virtual reality with artificial intelligence.

Keywords: Space Network, Voronoi Diagram, Delaunay Graph, Topology, Geometry, Integration

1. Introduction

The graph-based studies in architecture extend the scope of tangible space design through the intangible network of topological and geometric algorithms [e.g., 1]. In principal, the mathematical field of graph theory provides the algorithmic criteria for real life queries to be explored and resolved [e.g., 2]. Nevertheless, the application on architectural space relates the quantitative graph layout to the cognitive structure of visibility, navigation and human behavior in general [e.g., 3]. In this line of research, the proposed study raises the potential applicability of the Delaunay graph network in defining the integral structure of space design. The profound geometric resolution of the Delaunay graph forms a duality network with the Voronoi convex hull, which establishes the interdisciplinary platform where multilayered properties of space integration are embedded in virtual reality [4]. Meanwhile, the innovative artificial intelligence tools of programmed graph properties facilitate the virtual space processing and statistical analysis towards a unified approach of space integration [5].

The sample application selects the case study of historical roundabout Cairo for future conservation at the backbone of the metropolis. The geometric roundabouts represent a graph-like layout of generative round plazas with linking boulevards to form a satellite space pattern, which was designed in 1867 by the wellknown engineer 'Haussmann' of Parisian plan precedence and spread worldwide [6, 7]. However, the chronology of socioeconomic change has affected the integrity of roundabout Cairo, which suffers from the functional capacity of vehicular flow over walkability [8]. The lack of intangible spatial strategy leaves the radial network of old Cairo under the threat of piecemeal redevelopment [e.g., 9, 10, 11, 12]. Accordingly, this study focuses on the Delauany graph of roundabout Cairo with the objective of more algorithmic exploration towards the future space structure beyond visibility.

2. Methods

The other alternative methods than the Voronoi convex hull revolve around the graph criteria, which investigate the structure of architectural space in various network dimensions (Fig. 1). The fundamental method of space syntax constructs the topologic graph of axial and permeable principles to measure the integration of social networking in the layout configuration [13]. The essence

of social logic determines the magnitude of layout integration with the role of distributiveness for each space in ordinal sequence. The syntactic convex hull subdivides the contiguous open space into pixels of largest possible convex cells in the coordinate system. The resulted map converts the axial ray-shoot-monotone of the convex hull into a topological graph of axial line vertices with their intersections as connected. Despite the topology, the constructed base-map is geometric in nature by virtue of the shaped cell boundaries within the bound layout. However, the social objective diverts the emphasis of the space syntax method from the centroids of the geometric convex hull [14] to the generative line of outdoor sight along with the indoor interface and conovision of permeable human interaction in space [15]. Nevertheless, the enriching social method incorporated geometrical horizons of graph representation through the distinction of discursive and nondiscursive space formation [16, 17]. Further attempt revisited the geometrical convex hull of space syntax to integrate with geographic information systems and sciences [18]. The same social method extended to shape-grammar of re-structured graph representation from topologic towards geometry setup [19, 20, 21].

On the other, the generative geometry of shape-grammar defines the rules of computing space organization and solid formation in the design process [22, 23]. Since the process upholds social goals of function, the new strategies have integrated the syntactic logic into the grammar of shaping space [24, 25, 26]. In this regard, both topologic space syntax and geometrical shape grammar approach one another following the architectural theory of form follows function. Meanwhile, the modeling parameters of shape-grammar adopt the mathematical graph technique in various dimensions of the produced forms [e.g., 27, 28]. Also, the mathematical context of graph structure enabled the space syntax's methodical robustness such as the innovative syntactical synchronicity of building threshold through the outdoorindoor social logic along the pertained axial line criterion of graph representation [29]. So far in this line of research the basic mathematics of voronoi space with its dual delaunay graph geometry is less observed to have potential contribution to the network integrity of spatial structure and its formation morphology [e.g., 30, 31]. In this regard, the reciprocal autonomy of form follows function supposes the scientific voronoi-delaunay duality to conjoin the convex-graph structure of integral space at absolute scales of unlimited layout complexity. The initiative method defines the delaunay graph resolution where multivariate network modeling explores the integral space structure in parametric geometry and topology respective to form and function simultaneously. Practically, the case of roundabout Cairo is represented in delaunay graph to be explored in various geometric and topologic dimensions according to the parameters of; 1) universal distancing, 2) distributiveness, 3) delaunay moments and 4) traversable properties. Not only the correlative result reveals the holistic tangible and intangible structure of roundabout Cairo for future conservation but exemplifies the prospects of the delaunay graph for architectural space design with computable artificial intelligence as well.

3. Results

3.1. Universal Distance

The issue of universal distance investigates the measured distance from one graph generator to all others of the spatial system in extended scope of spatial analysis [e.g., 32]. The aggregation of travelled distances compares the layout structure of graph generators with the shortest synonymous to the most integral of the layout (Fig.2 & Table 1). The result determines generator-9 to have the shortest distance of visiting all others along the delaunay network. In contrast, generator-13 elongates in furthest extent of the layout. Between the two extremes several observations are pointed out for the integral structure. The global structure integrates the pyramidal-mold of generator-7 at the apex down to the base of generators 11 & 12 in closest variance to layout average of universal distancing. True moderation of molded layout structure carries the sub-network of dense zigzagging structure up to the apex in shortest distances. Meanwhile, the same mold attaches the most distant generators 13, 14 & 15 at two stretching wings from sides of the global pyramidal containment. Minor structure, nevertheless, shifts the global base into subpyramidal containment at generators 9 & 4 where the highest distancing integrity locates. Further base shifting to generators 8 & 6 continues the global integrity in top-tier rank of shortening distance. Therefore, the universal distance defines one large triangulation composed of smaller ones and reaches out to distant tips from sides with the whole integrated through the sub-base of generator-9 in shortcuts.

At the detailed resolution of global structure, generator-9 connects direct to generators 2, 3 & 5 which are characterized by their location inside the pyramid of global triangulation. In particular, generator-3 is ranked second after generator-9 and followed in the ordinal ranks by generators 5 & 2 respectively. Privilege of generator-3 forms a wider network of loops towards the global base whereas generator-5 has more limitation at the apex. Universal distance of generator-5, however, acquires a higher rank than generator-2 of more drifting from centrality at the global structure. On the other, generator-8 competes in better position of sandwich-rank between generators 5 & 2 with only connectivity to generator-5 among the pyramidal inner generators. In this regard, the inner generators are regarded as dummy-generators of subordinate structure to the ones at the global pyramidal boundary in highest layout integrity by distance. Justified top-rank of generator-9 connects to all of these dummies in comparison to the lower rank of neighboring generator-8 of single inner connectivity at the squeezed apex.

Comparable structure of generator-4 connects to two of the inner generators, in addition to generator-9 of shared middle base in pyramidal overlay to the global. Despite this fact, the sole structure of generator-4 at the middle of the hypotenuse affects its distance measure in longer travel when compared to the opposite side of multiple generators aligned in close proximity and centered by generator-9. In fact, this structure benefits more generator-9 to network through generator-4 of shortcut to the furthest wing in

shortest distance possible, but generator-4 has to cross more generators passing through generator-9 or the inner ones on the way to others nearby. Overview of one-way distancing structure adds generator-4 to the dummies of generator-9 but not the inverse as proved by the universal distance. Similar network of generator-6 does for generator-8 same as generator-4 for generator-9 in dummy structure. Both generators 8 & 5 benefit from this structure to connect to the long wing in shortcut of generator-6, but the inverse holds untrue. Distant from the global pyramid, the pseudo disintegration of generator-13 forms another dummy connection to generator-14 in one of the shortest distances found at the layout level. It forms a unique symbolic structure at the spot of Cairo Citadel apart from all others, while in the meantime delegates the layout integrity to the shadow generator-14 of shortest variance from the other tip of generator-15, thus the overall balanced distance structure.

3.2. Distributiveness

Geometrical delaunay graph allows topological measure of spatial distributiveness to measure the relative asymmetry of each generator in comparison to all others of the layout (Table 2). While the graph generation of delaunay triangulation differs from the convex mapping of space syntax, the same statistical measure of relative asymmetry applies to both or any other given graph layout of spatial system. As a rule of thumb, the lesser value of relative-asymmetry the more distributiveness of generative space integration. The statistical measurement is formulated as: Relative asymmetry $(\mathrm{RA}) = \frac{2\,(\mathrm{MD}-1)}{\mathrm{K}-2}$, where 'MD' is the mean depth of a space and 'K' is the number of spaces in the spatial system [13, p.108]. The RA measurement depends on the depth structure of each vertex in relationship to all others as per the topological length rather than distance. Justified graph representation arranges the vertices in topped-up levels of depth from any one vertex to the rest in connection. The depth measure determines the relative asymmetry of the global layout in overall spatial integration in addition to the integral structure of each space with respect to the whole layout integrity and in relationship to others as well. Applying the depth measure of distributiveness on the delaunay graph determines the integral structure at different network resolutions.

The resulted RA has an overall integral structure of highly distributed structure with mean depth varying from 1.57 to 2.43 among generators. The lowest RA value of the most integral space determines generator-9 in extreme distributiveness throughout the layout connectivity. Its justified graph keeps at level-2 of all looping bushy-structure except the length-3 depth of generator-13 in single-loop at top. The second-rank identifies generator-4 of close RA value to the top-rank with only one swap between the first and second levels of the justified graph. Further third-rank of generator-2 has a one more swap connectivity of length-3 with a little effect on the layout integrity in comparison to the top two. Following generator-12 has exactly the same RA as generator-2 in repeated-rank of integration but of changed strategy by more investment in length-1 connectivity in compensation to the increased third-level of the justified graph. Intensified connectivity of middle length-2 in justified graph of generator-3 corresponds to just above average layout integrity at fifth-rank of distributiveness. The approached layout average extends to generators 8 & 10 of exactly the same RA value as generator-3 but of varied depth levels. The latter two, nevertheless, are isomorphic through exchanged depth of graph vertices to end up of equal justification. Just below average integration expands into four similar RA values of generators 5, 6, 14 & 15. Again, isomorphic graphs of generators 5 & 14 are distinctive and differ from the other two. Added level-4 connectivity of generator-15 is met with more investment at the first two levels, whereas generator-6 demonstrates the most stable connectivity of homogenous structure along the three depth levels.

The bottom range of layout integrity starts by generator-1 having one more level-2 connection over the previous homogenous distribution at average. Less distributiveness of generator-7 minimizes the level-1 depth of shifted connectivity to more level-2 and more level-3 as well. More deep structure of generator11 has more level-3 connects over level-2 for the first time of the layout to disintegrate. The most disintegration of layout by generator-13 extends to the fourth length of connectivity with optimum networking at level-3 of the justified graph. Therefore, the high integrity of global layout with optimal distributiveness and loops everywhere demonstrates some variance of depth measures among the justified graphs of individual generators. The global structure of topologic length compares and contrasts with the geometric distance by both extremely direct and inverse relationships as well. Top-tier integrity enforces generator-9 by both distancing and relative asymmetry integral structure. Similarly, the least integration corresponds to generator-13 by both measurements. In contrast, effective generators change the layout networking of dual structure such as generator-4 from decreasing universal distance to the top distributiveness with generator-9 in connection. On the contrary, inner generators 3 & 5 change from catalyst universal distancing in top-tier to just about average relative asymmetry of less integration.

3.3. Delaunay Moments

Moments of delaunay graph concern the measurements of pure geometrical characteristics as formed by each triangulation. One of the major interests is the circumcircle property where the three-generators of each triangle draw a circle that passes through them and without containing any other vertex of the layout (Fig. 3 & Table 3). The resulted geometry defines the geometrical structure in various dimensions such as the circumcenter equidistant to the triangular generators, the rayshoot-monotone of visibility dimension, the territories of each group with their overlap, the circular area and shortest perpendicular distance to the triangular edges. Starting by the circumcenter, more than half of the layout triangles have their circumcenter located outside of the triangular boundaries. Among all generators only generator-1 has all circumcenter points located inside their respective triangles. Complete autonomy Cairo enforces the triangulations of generator-1 in relationship to the whole layout structure. Similarly, the innermost triangulation of

generators 3, 4 & 9 contains the circumcenter and spread in waves of further selective triangulations with generators 2 & 10 holding the same containment property. Meanwhile, unique containment by the single triangulation 6, 7 & 8 without overlap to others of the same property forms a distinctive structure at the layout apex. Apart from this, the majority of triangulations have their circumcenters located outside the circumcircles of drifted meeting point per triangular group.

The visibility dimension examines the line of sight along the ray directions passing through the circumcircles in largest number possible of ray-shoot-monotone property. The conceptive property is paralleled by the comparable but different axial mapping and isovist scope of visibility in extended analytics of space syntax [e.g., 33]. Superimposed ray-shoot on the circumcircles stretches the visibility in more cognitive structure. Two major directions of vertical and horizontal axes satisfy the property in different dimensions. Several trials of horizontal rays cut through the dense overlapping circmcircles in maximum 8 or 9 penetrations along two parallel shoots. The vertical trials, nevertheless, are longer in single shoot of eccentric spacing. In this regard, the horizontal shoot is more visible and comprehensive with go-and-return duality in contrast to the vertical crossing of segmented one-way shot. Different ray, however, sets generator-15 in concentric waves of one shoot to infinity. Meanwhile, the generator-circumcenter equidistance of each triangle compares their triple-tying structure. The shortest equidistance belongs to the triangle (5, 6, 8) of exterior location however. The same structure observes triangle (5, 8, 9) of top-tying equidistance as well. Further two triangles (1, 10, 11) and (1, 2, 10) tie in similar rank with internal circumcenter though. The remaining triangles are more stable with the innercenters dominating towards the average distance and followed by outer-centers down to bottom. The toptier symbolic structure, thus, maintains the proximity of either inner or outer equidistant spots in common.

In another projection from the circumcenter to the triangular sides, the distance varies in comparison within each triangle and among the triangles as well. The shortest projection continues the mix of outerinner centralization in top-tier proximity towards one triangular side only. The other two sides of longer projections have more tendencies to cluster the triangles into higher proximity of interior centres against the exterior crossover. One exception is the shared two triangles of generators 5 & 8 that belong to the cluster of interior-point while having an exterior reach. Meanwhile, the specific triangle (4, 12, 14) has interior-center but joins the other external cluster. More specific triangulation of generator-1 keeps stable in top-tier along all clustering differences, thus holding top-rank of overall mean-distance projection. Constant bottom-rank, nevertheless, sets the triangles of generators 13 & 15 in distant projections to any of its sides. The circumcircling results impact on the angles of triangulation with further clustering observation. The narrowest two angles below average form a clear cluster of triangles having external circumcenter. The third widest angle, however, flips the cluster to triangles of internal centers. Meanwhile, the length of triangular sides changes the clustering into shortest and longest lengths of exterior circumcenter, whereas the upper-medium lengths are dominated by internally centered triangles. The same clustering extends to the area and perimeter with their ratio in confirmation. Therefore, moments of delaunay graph set isosceles-triangles of internal circumceneter having coherent relationships of generators, but the obtuse-triangles have extroverted tendency of wider networking in compensation.

3.4. Delaunay Traversing

Traversable properties of delaunay graph track the possible visit once to all generators and/or edge links in a walk that may or may not return to the start point. Three major tracks of hamiltonian, traversable and eulerian properties to explore. Starting by the hamiltonian algorithm of finding the path or circuit to pass by the total vertices without repetition of any in sequence. Graph theory defines one satisfactory condition as: *"If G is a graph of order p (≥ 3) such that deg v ≥ p/2 for every vertex v of G, then G is Hamiltonian."* [34, p.69] Otherwise the graph has to be examined by try-and-error exploring for proof. Applying the algorithm on the delaunay graph is not guaranteed by the stated condition due to less links than half of the vertices per each. Checking the network from anyone vertex there is always a route path that links all vertices without revisiting any of them and ends up at the same location. For example, starting from the very inner generator-5 one can take the route of 5-8-7-6-14-13-12-4-3-2-10-1-11-15-9-5 in sequence regardless of distancing and shortcuts. Similarly, from the furthest outer generator-13 the route exists as 13-12-1-2-3-4-5-8-9-10-11-15-7-6-14-13 in complete circuit. Accordingly, the highly connected delaunay graph proves not only hamiltonian path but circuit as well. It affords walkability dimension of spatial integration for a human or vehicle to travel across the spatial system of roundabouts in full excursion and drop at the same spot. The property satisfaction from any vertex optimizes the variety of choice with homogenous structure of spatial integration for the first time of the whole layout.

Changing the excursion to the traversable property that is directly related to the eulerian one identifies if it is possible to trail all of the edges in sequence without duplication of any. If this traversable trail exists then the network is also eulerian in path but not necessarily circuiting. In firm condition *"A multigraph G is traversable if and only if G is connected and has exactly two odd vertices. Furthermore, any eulerian trail of G begins at one of the odd vertices and ends at the other odd vertex."* [34, p.58] Meanwhile, the network is eulerian in circuit if and only if: *"A multigraph G is eulerian if and only if G is connected and every vertex of G is even."* [34, p.55] Beginning with the traversable condition, the delaunay graph proves to be non-traversable where it is not possible to cross all links once in order simply because it exceeds two odd vertices for the excursion to start and end at. By default, the network is not eulerian in path and of course circuit as well. Despite this conditional fact, several trails clarify the extent to which the graph is traversable. Any two generators can be linked in various traversable trails of shortcuts in minimum

length or choose elongated trails of maximized length. The same applies to minor circuits among generators at eulerian circuit of specific destinations. Seen from this viewpoint the network focuses on minor graphs of eulerian and traversable trails, while in the meantime achieves major hamiltonian circuiting allover. In this regard, the spatial system allows the integration of roundabouts in major explicit phenomenon through interactive links of major choice in graph minors.

Further application of graph minor may reduce the spatial system in contracted graph characteristics. For triangulation, the global cycling system of the delaunay graph may contract each cycle to become a uni-vertex representing each triangle in connection to its neighbors (Fig. 4). The resulted graph expands the triangular relationships into larger cycles in less number. The largest cycle centered by generator-9 connects to all cycles in highest distributiveness of the contracted layout. Meanwhile, generator-13 forms the only tail of the contracted layout in lowest integrity. This tail, however, connects to the second integral cycle of generator-4 in layout compensation. This tail, however, causes the layout to lose the hamiltonian circuiting but still holds true path. Further contraction of this tail returns the layout to hamiltonian circuit at any point. The traversable and eulerian properties, nevertheless, keep functioning as graph components with single eulerian cycle at a time. Therefore, the original graph and its minor demonstrate cross-correlation of their extreme integral structure by generators 9 & 13, in addition to minor traversing properties of the major counterpart.

4. Discussion

Discussion of the delaunay graph encapsulates geometrical, topological and algorithmic properties in one layout of spatial structure. Identifying the issue of structured space integration, in particular, justifies the role of individual generators and components at different resolutions of the global system. The crosscorrelation of various quantitative graph dimensions clarifies the global system of interactive layout for strategic enforcement. Correlative multivariate strategy of space through the media of delaunay graph in dual voronoi diagram shifts the layout structure into the realm of virtual reality and beyond visibility. The voronoi graphing of computable tools in artificial intelligence further shifts the virtual realm into imaginary field of creative layout. Meanwhile, virtual imagination has been realized in programmable computation of graphs and networks to create and analyze [e.g., 35, 36]. Having the method and its tools to compute may afford the platform of graph network into the future space. One application on the historical case of roundabout Cairo in delaunay graph has revealed new invisible dimensions of the layout structure to strategize for future conservation. Realizing the imaginary graph strategy on ground requires further processing to compare the graph results with the existing network for readjustment breakthrough or strategize when creating new. While the roundabouts are predefined in real as-built Cairo and in graph generators as well, the strategy is required for their links that may vary from one real situation to the other as from one layer of graph property to the other, thus the interactive links. In Cairo reality the existing network of links is not limited to the roundabout direct linkages but extends in all directions for the layered strategies to be enabled, interactively, upon the delaunay conclusions.

5. Conclusions

The study first proposed the delaunay graph network to correlate form and function in one model of parametric design for architectural space methodology. The method is verified not as new to the field but as an already existing basic-science that can be applied to any kind of space, though not fully experienced for the architectural space design as is yet to come. Secondly, the study applied the delaunay graph on the historical plan of roundabout Cairo for the future purpose of conserving its integral space structure. The criteria of applied delaunay modeled the roundabout network as per the topological and geometric integral measurements of universal distance, distributiveness, moments and traverse properties. The results crosscorrelate the original integrity of roundabout Cairo as follows:

1. The global structure of spatial integration forms one large triangle composed of smaller triangulations in shortest universal distance towards the central zone. The topologic distributiveness correlates to the geometrical distance with interactive integral ranks among the central generators. Specifically, generator-4 swaps the geometric-topologic integrity with the surrounding central ones to form a catalyst zone of the global system. Further geometric moments enforce the global triangular structure of dense ray-shoot and circumcircle properties, in addition to generator-1 of more geometrical integrity at the triangular base. Nevertheless, the global structure satisfies the absolute integrity of hamiltonian circuiting, which continues at the minor graph of single node per triangulation.
2. The extreme layout integration determines generator-9 in top rank of shortest distance and distributive structure, which is further enforced in graph minor and traversable strategies of largest cycling space. The top integral role multiplies through the direct connectivity to generators 3, 4 & 5 at the catalyst central zone, which boosts the highest distributiveness of the layout in chain reaction. Nevertheless, the moments of triangulation set the same generator in densest circumcircling of maximal degree links and cycles of various integral ranks, which improves the shared integrity with generators of all ranks and not only the central top-tier. Disseminating this global integrity towards non-distributive and distant triangulation of distorted moments affords for others as of generator-1 to be locally stable.
3. The least integrity, however, determines generator-13 of the longest universal distance and the lowest distributiveness of the layout with skewed moments of triangulation. Despite these deficiencies, its close ties to generator-14 blend their integral outlet along all graph measurements, which globally levels up to the better connectivity of the single generator-15 at the layout's opposite tip. The same two generators when seen as one illuminates the only tail found at the graph minor of triangulation, thus the totally cyclic spaces of global integration. In functional terms, the

landmark structure of Cairo Citadel corresponding to generator-13 stands tall among all others in symbolic depth of layout.

Declaration of Interests

The research paper declares to have no known competing financial interests or personal relationships that could have appeared to influence the work reported.

References

1. Blanchard, P., & Volchenkov, D. (2009). *Mathematical analysis of urban spatial networks*. Springer.
2. Diestel, R. (2006). Graph theory. (3rd ed.), Springer, Berlin.
3. Franz, G., Mallot, H., & Wiener, J. (2005) Graph-based models of space in architecture and cognitive science: a comparative analysis, In Leong, Y. (Ed.), Architecture, Engineering and Construction of Build Environments, Windsor, ON, Canada: *International Institute for Advanced Studies in Systems Research and Cybernetics*, 30-38.
4. Okabe, A., Boots, B., Sugihara, K., & Chiu, S. N. (2000). Spatial tessellations: concepts and applications of Voronoi diagrams. (2nd ed.), John Willy & Sons, Chichester.
5. Wolfram, S. (2003). *The mathematica book.* Wolfram Research, Inc..
6. Mubarak, A. (1889). Khetat. Beaulac Press, Cairo. (In Arabic)
7. El Shazly, A. E. (2019). The Future of the 'Insurance Plan'in Cairo and Alexandria. In *Conservation of Architectural Heritage: A Culmination of Selected Research Papers from the Second International Conference on Conservation of Architectural Heritage (CAH-2), Egypt 2018* (pp. 9-22). Springer International Publishing.
8. El-Shazly, A. E. (2003). The Prospects of the 'European Quarter'in Cairo. *Journal of Asian Architecture and Building Engineering, 2*(1), 175-182.
9. Attia, S. (2012). Revitalization of Downtown as center for social democracy and sustainable growth. *Ecocity Summit Book Library.*
10. The Town Planning Department & Cairo University (2002). The European Quarter of Cairo: A Study in conservation, Final Report, Published by the Town Planning Department, Cairo.
11. Volait, M. (2001). *Le Caire, Alexandrie, Architectures européennes, 1850-1950.* Presses de l'IFAO.
12. Scharabi, M. (1989). *Kairo: stadt und architektur im zeitalter des europäischen kolonialismus*. Wasmuth.
13. Hillier, B., & Hanson, J. (1984). *The social logic of space*. Cambridge University Press.
14. Osmond, P. (2011). The convex space as the'atom'of urban analysis. *The Journal of Space Syntax, 2*(1), 97-114.
15. Hanson, J. (1998). *Decoding homes and houses*. Cambridge University Press.
16. Hillier, B. (1996). Space is the machine. Cambridge University Press.
17. Hillier, B., Turner, A., Yang, T., & Park, H. T. (2010). Metric and topo-geometric properties of urban street networks: some convergences, divergences, and new results. *Journal of Space Syntax, 1*(2), 258-279.
18. Jiang, B., & Claramunt, C. (2002). Integration of space syntax into GIS: new perspectives for urban morphology. *Transactions in GIS, 6*(3), 295-309.
19. Lee, J. H., Ostwald, M. J., & Gu, N. (2016). A justified plan graph (JPG) grammar approach to identify spatial design patterns in an architectural style. *Environment and Planning B: Urban Analytics and City Science, 45*(1), 67-89.
20. Lee, J. H., Ostwald, M. J., & Gu, N. (2017). A Combined plan graph and massing grammar approach to frank lloyd wright's prairie architecture. *Nexus Network Journal, 19*, 279-299.
21. Lee, J. H., Ostwald, M. J., & Gu, N. (2013). Combining space syntax and shape grammar to investigate architectural style: Considering Glenn Murcutt's domestic designs. In *Proceedings of the Ninth International Space Syntax Symposium, Seoul, Republic of Korea* (Vol. 31, pp. 5.1–5.13).
22. Tching, J., Reis, J., & Paio, A. (2013, June). Shape grammars for creative decisions: In the architectural project. In *2013 8th Iberian Conference on Information Systems and Technologies (CISTI)* (pp. 1-6). IEEE.
23. Benrós, D., Duarte, J. P., & Hanna, A. (2012). A new palladian shape grammar: A subdivision grammar as alternative to the palladian grammar, *International journal of architectural computing, 10*(4), 521-540.
24. Heitor, T., Duarte, J. P., & Pinto, R. M. (2003). Combining grammars and Space Syntax: Formulating, evaluating, and generating designs. In *Proceedings of the Fourth International Space Syntax Symposium, London: University College London* (Vol.1, pp.28.2–28.18).
25. Eloy, S., & Guerreiro, R. (2016). Transforming housing typologies. Space syntax evaluation and shape grammar generation. *Transforming housing typologies. Space syntax evaluation and shape grammar generation*, (15), 86-114.
26. Cicek, S., & Turhan, G. D. (2022). Computational generation of a spatial layout through syntactical evaluation and multi-objective evolutionary optimization. *International Journal of Architectural Computing, 20*(3), 610-629.
27. As, I., Pal, S., & Basu, P. (2018). Artificial intelligence in architecture: Generating conceptual design via deep learning. *International Journal of Architectural Computing, 16*(4), 306-327.
28. Kobayashi, Y., Katoh, N., Okano, T., & Takizawa, A. (2015). An inductive construction of rigid panel-hinge graphs and their applications to form design. *International Journal of Architectural Computing, 13*(1), 45-68.
29. Dawes, M. J., & Ostwald, M. J. (2021). Space syntax: mathematics and the social logic of architecture. In *Handbook of the Mathematics of the Arts and Sciences* (pp. 1407-1418). Cham: Springer International Publishing.
30. El Shazly, A. E. (2019). On the Spatial Conservation of Roundabout Cairo Using Pitteway Graph. In *Conservation of Architectural Heritage: A Culmination of Selected Research Papers from the Second International Conference on Conservation of Architectural Heritage (CAH-2), Egypt 2018* (pp. 23-36). Springer International Publishing.

31. El Shazly, A. E. (2022). Prospects of room graph at 'Seqina'slum in Egypt. *Ain Shams Engineering Journal, 13*(3), 101594.
32. Otto, F. (2003). *Occupying and connecting* (Vol. 3). Fellbach, Germany: Edition Axel Menges.
33. Turner, A., & Penn, A. (1999, March). Making isovists syntactic: isovist integration analysis. In *2nd International Symposium on Space Syntax, Brasilia* (pp. 103-121).
34. Chartrand, G. (1977). *Introductory graph theory*. Courier Corporation.
35. *https://reference.wolfram.com/language/guide/GraphsAndNetworks.html* (May 7th, 2024)
36. Pemmaraju, S., & Skiena, S. (2003). *Computational discrete mathematics: Combinatorics and graph theory with mathematica®*. Cambridge university press.

Appendix of Tables

Gen	1	2	3	4	5	6	7	8	9	10	11	12	13	14	15	UD (Km)
1	0.00	0.41	0.75	1.00	1.43	1.55	1.78	1.31	0.99	0.42	0.26	0.72	2.55	2.30	2.06	17.51
2	0.41	0.00	0.34	0.59	1.02	1.14	1.39	0.93	0.61	0.35	0.67	0.66	2.49	2.17	1.86	14.62
3	0.75	0.34	0.00	0.25	0.68	0.80	1.24	0.78	0.45	0.68	1.01	0.78	2.18	1.84	1.86	13.63
4	1.00	0.59	0.25	0.00	0.43	0.55	0.99	0.66	0.48	0.94	1.26	0.95	3.41	1.58	1.85	14.94
5	1.43	1.02	0.68	0.43	0.00	0.16	0.60	0.23	0.44	1.01	1.38	1.38	2.31	1.97	1.31	14.33
6	1.55	1.14	0.80	0.55	0.16	0.00	0.44	0.33	0.60	1.17	1.54	1.49	2.15	1.81	1.31	15.02
7	1.78	1.39	1.24	0.99	0.60	0.44	0.00	0.46	0.79	1.36	1.73	1.93	2.59	2.25	0.87	18.41
8	1.31	0.93	0.78	0.66	0.23	0.33	0.46	0.00	0.32	0.89	1.27	1.56	2.48	2.14	1.08	14.44
9	0.99	0.61	0.45	0.48	0.44	0.60	0.79	0.32	0.00	0.57	0.94	1.27	2.40	2.06	1.25	13.17
10	0.42	0.35	0.68	0.95	1.01	1.17	1.36	0.89	0.57	0.00	0.37	1.00	2.83	2.58	1.64	15.82
11	0.26	0.67	1.01	1.26	1.38	1.54	1.73	1.27	0.94	0.37	0.00	0.98	2.81	2.56	1.94	18.69
12	0.72	0.66	0.78	0.95	1.38	1.49	1.93	1.56	1.27	1.00	0.98	0.00	1.83	1.58	2.51	18.63
13	2.55	2.49	2.18	3.41	2.31	2.15	2.59	2.48	2.40	2.83	2.81	1.83	0.00	0.34	3.46	33.82
14	2.30	2.17	1.84	1.58	1.97	1.81	2.25	2.14	2.06	2.58	2.56	1.58	0.34	0.00	3.12	28.30
15	2.06	1.86	1.86	1.85	1.31	1.31	0.87	1.08	1.25	1.64	1.94	2.51	3.46	3.12	0.00	26.09
Av.	1.17	0.97	0.91	1.00	0.96	1.00	1.23	0.96	0.88	1.05	1.25	1.24	2.25	1.89	1.74	18.49

Table 1: Universal Distance of Delaunay Graph

Gen.	1	2	3	4	5	6	7	8	9	10	11	12	13	14	15	Deg.	MD	RA
1	0	1	2	2	3	3	3	3	2	1	1	1	2	2	2	4	2	0.153846
2	1	0	1	2	2	3	3	2	1	1	2	1	2	2	2	5	1.785714	0.120879
3	2	1	0	1	2	2	3	2	1	2	3	1	2	2	2	4	1.857143	0.131868
4	2	2	1	0	1	1	2	2	1	2	3	1	2	1	2	6	1.642857	0.098901
5	3	2	2	1	0	1	2	1	1	2	3	2	3	2	2	4	1.928571	0.142857
6	3	3	2	1	1	0	1	1	2	3	3	2	2	1	2	5	1.928571	0.142857
7	3	3	3	2	2	1	0	1	2	2	2	3	3	2	1	3	2.142857	0.175824
8	3	2	2	2	1	1	1	0	1	2	2	3	3	2	1	5	1.857143	0.131868
9	2	1	1	1	1	2	2	1	0	1	2	2	3	2	1	7	1.571429	0.087912
10	1	1	2	2	2	3	2	2	1	0	1	2	3	3	1	5	1.857143	0.131868
11	1	2	3	3	3	3	2	2	2	1	0	2	3	3	1	3	2.214286	0.186813
12	1	1	1	1	2	2	3	3	2	2	2	0	1	1	3	6	1.785714	0.120879
13	2	2	2	2	3	2	3	3	3	3	3	1	0	1	4	2	2.428571	0.21978
14	2	2	2	1	2	1	2	2	2	3	3	1	1	0	3	4	1.928571	0.142857
15	2	2	2	2	2	2	1	1	1	1	1	3	4	3	0	5	1.928571	0.142857

Table 2: Distributiveness of Delaunay Graph

Tria.(Km)	Circ.A.	G	E1	E2	E3	M-E	A1	A2	A3	L1	L2	L3	M-L	Tri. A.	Per.	A/P
(1,10,11)	0.15	0.21	0.04	0.10	0.17	0.07	37	62	81	0.27	0.39	0.44	0.36	0.05	1.09	0.05
(1,2,10)	0.17	0.24	0.10	0.10	0.15	0.08	49	65	66	0.36	0.43	0.44	0.41	0.07	1.23	0.06
(1,2,12)	0.45	0.38	0.07	0.15	0.31	0.13	35	65	80	0.43	0.68	0.75	0.62	0.15	1.86	0.08
(2,9,10)	0.32	0.32	0.07	0.13	0.27	0.11	34	68	78	0.36	0.59	0.63	0.53	0.10	1.59	0.07
(2,3,9)	0.34	0.32	0.07	0.22	0.28	0.14	32	47	101	0.35	0.47	0.63	0.48	0.08	1.45	0.05
(2,3,12)	0.50	0.41	0.06	0.22	0.38	0.16	24	57	99	0.35	0.68	0.81	0.62	0.12	1.85	0.06
(3,4,9)	0.18	0.25	0.04	0.09	0.21	0.08	31	69	80	0.26	0.47	0.50	0.41	0.06	1.23	0.05
(3,4,12)	0.98	0.57	0.31	0.32	0.56	0.28	13	44	123	0.26	0.81	0.98	0.69	0.09	2.06	0.04
(4,5,9)	0.21	0.27	0.11	0.14	0.15	0.10	56	57	67	0.45	0.45	0.50	0.47	0.09	1.40	0.07
(4,5,6)	0.43	0.36	0.24	0.29	0.36	0.21	13	37	130	0.17	0.45	0.57	0.39	0.03	1.18	0.02
(4,6,14)	2.83	0.97	0.25	0.52	0.92	0.40	17	58	105	0.57	1.65	1.88	1.37	0.46	4.10	0.11
(4,12,14)	2.22	0.85	0.24	0.27	0.70	0.29	35	72	73	0.98	1.64	1.65	1.43	0.77	4.28	0.18
(5,8,9)	0.15	0.22	0.06	0.15	0.20	0.10	31	46	103	0.24	0.34	0.45	0.34	0.04	1.03	0.04
(5,6,8)	0.11	0.20	0.08	0.15	0.18	0.10	26	37	117	0.17	0.24	0.35	0.25	0.02	0.75	0.02
(6,7,8)	0.20	0.25	0.08	0.10	0.18	0.09	44	66	70	0.35	0.46	0.48	0.43	0.08	1.29	0.06
(7,8,15)	0.98	0.57	0.14	0.36	0.52	0.24	24	51	105	0.48	0.90	1.12	0.84	0.21	2.51	0.08
(8,9,15)	1.54	0.71	0.31	0.45	0.70	0.35	14	51	115	0.34	1.12	1.30	0.92	0.17	2.76	0.06
(9,10,15)	3.14	1.02	0.57	0.78	0.98	0.56	17	39	124	0.59	1.30	1.70	1.20	0.32	3.60	0.09
(10,11,15)	7.07	1.54	1.16	1.27	1.53	0.94	7	34	139	0.39	1.70	2.01	1.37	0.21	4.11	0.05
(12,13,14)	4.99	1.29	0.88	1.01	1.29	0.76	8	39	133	0.35	1.64	1.90	1.30	0.21	3.90	0.05
Av.	1.35	0.55	0.24	0.34	0.50	0.26	27.35	53.20	99.45	0.39	0.82	0.96	0.72	0.17	2.16	0.07

Table 3: Moments of Delaunay Graph

Appendix of Figures

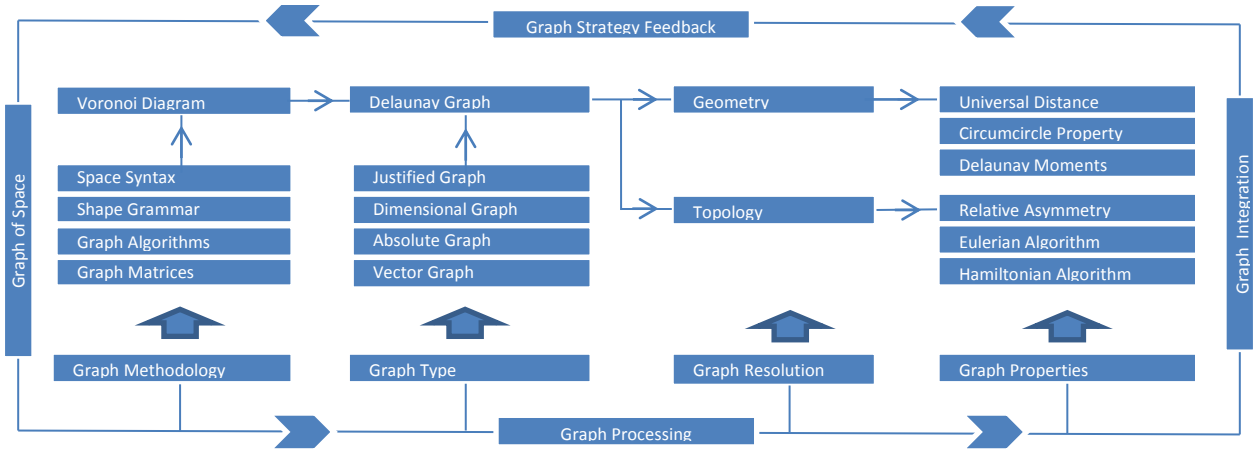

Figure 1: Flow Chart of Space Graph

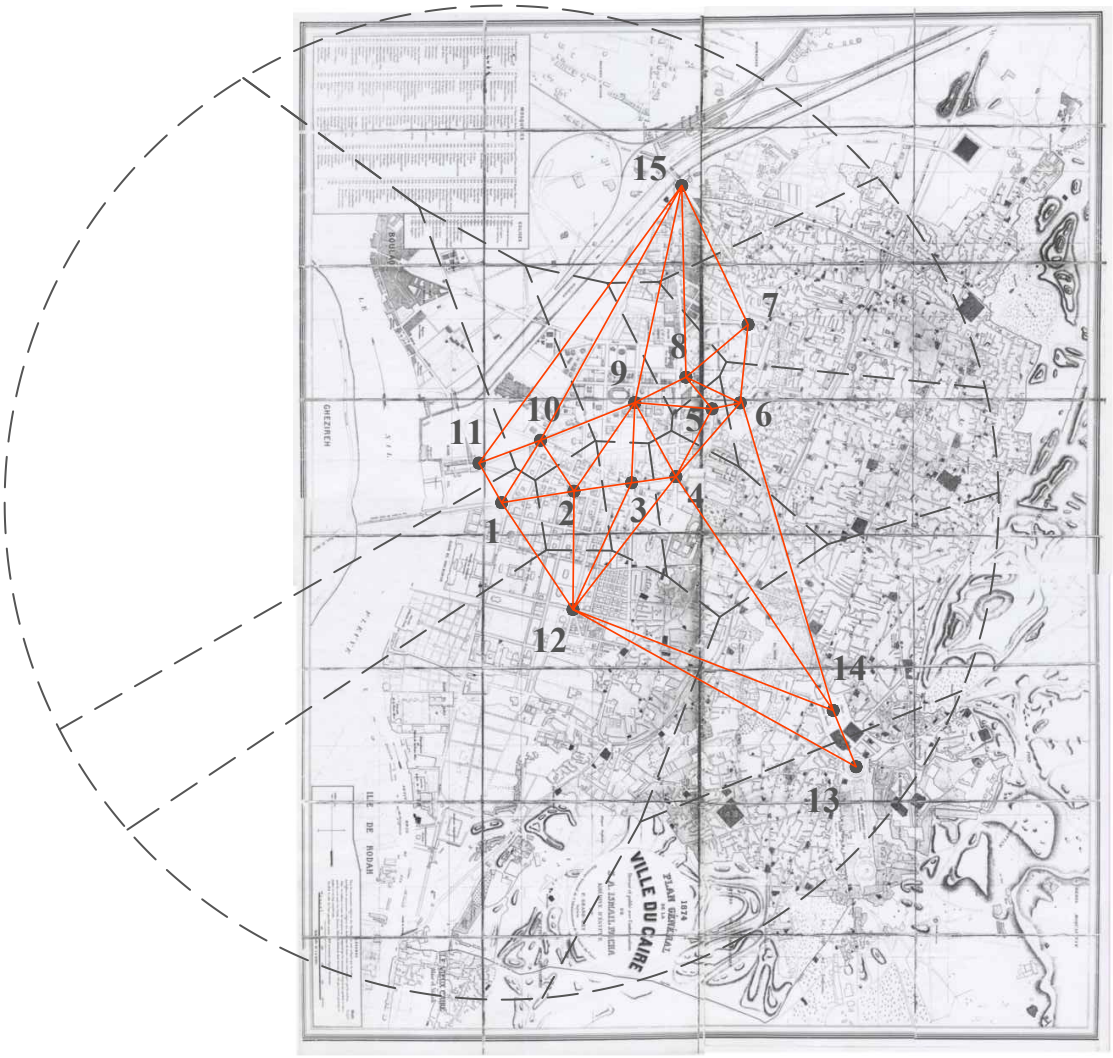

Figure 2: Delaunay Graph of Roundabout Cairo
(Source of Basemap: A copy from the Survey Department, Cairo)

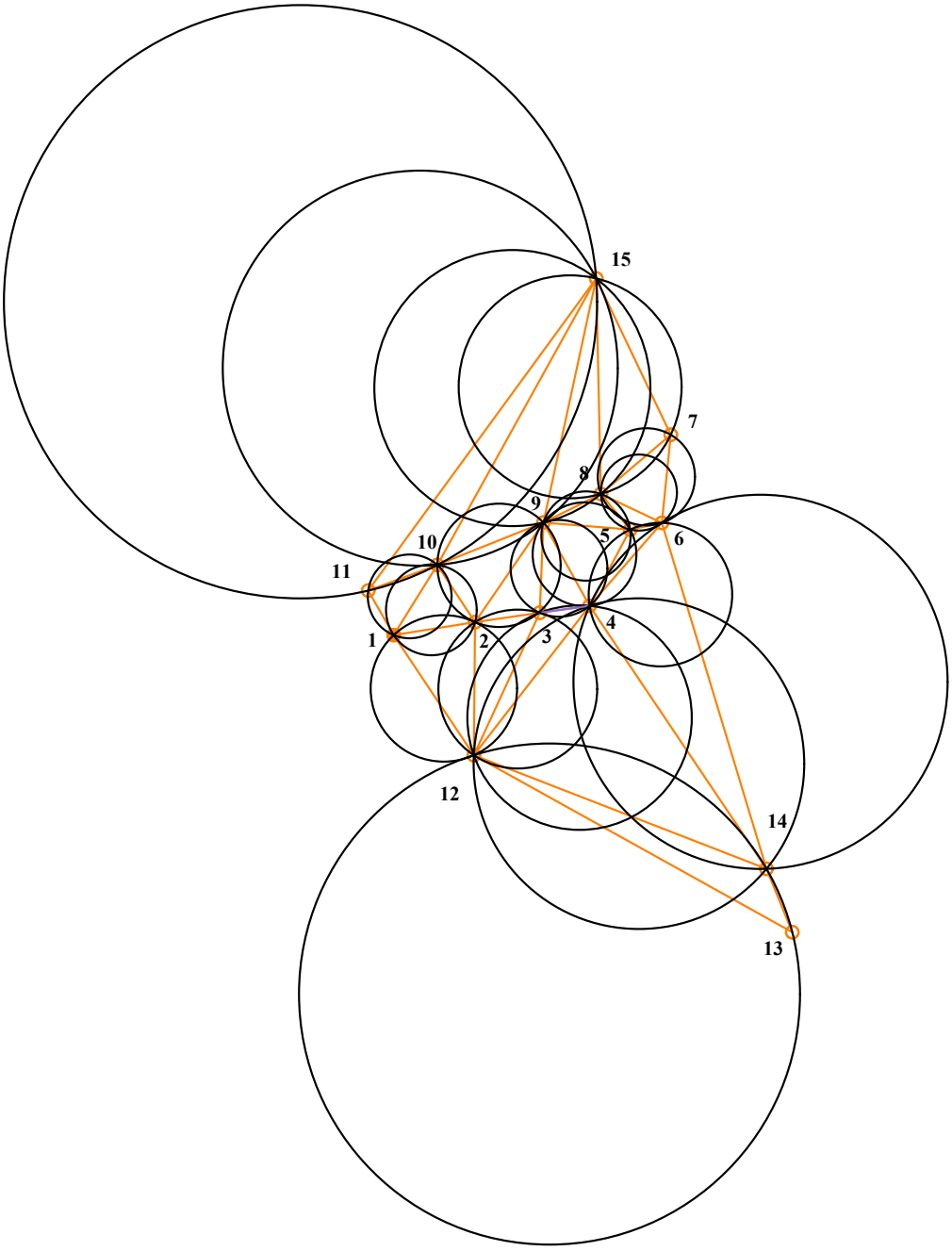

Figure 3: The Circumcircles of Roundabout

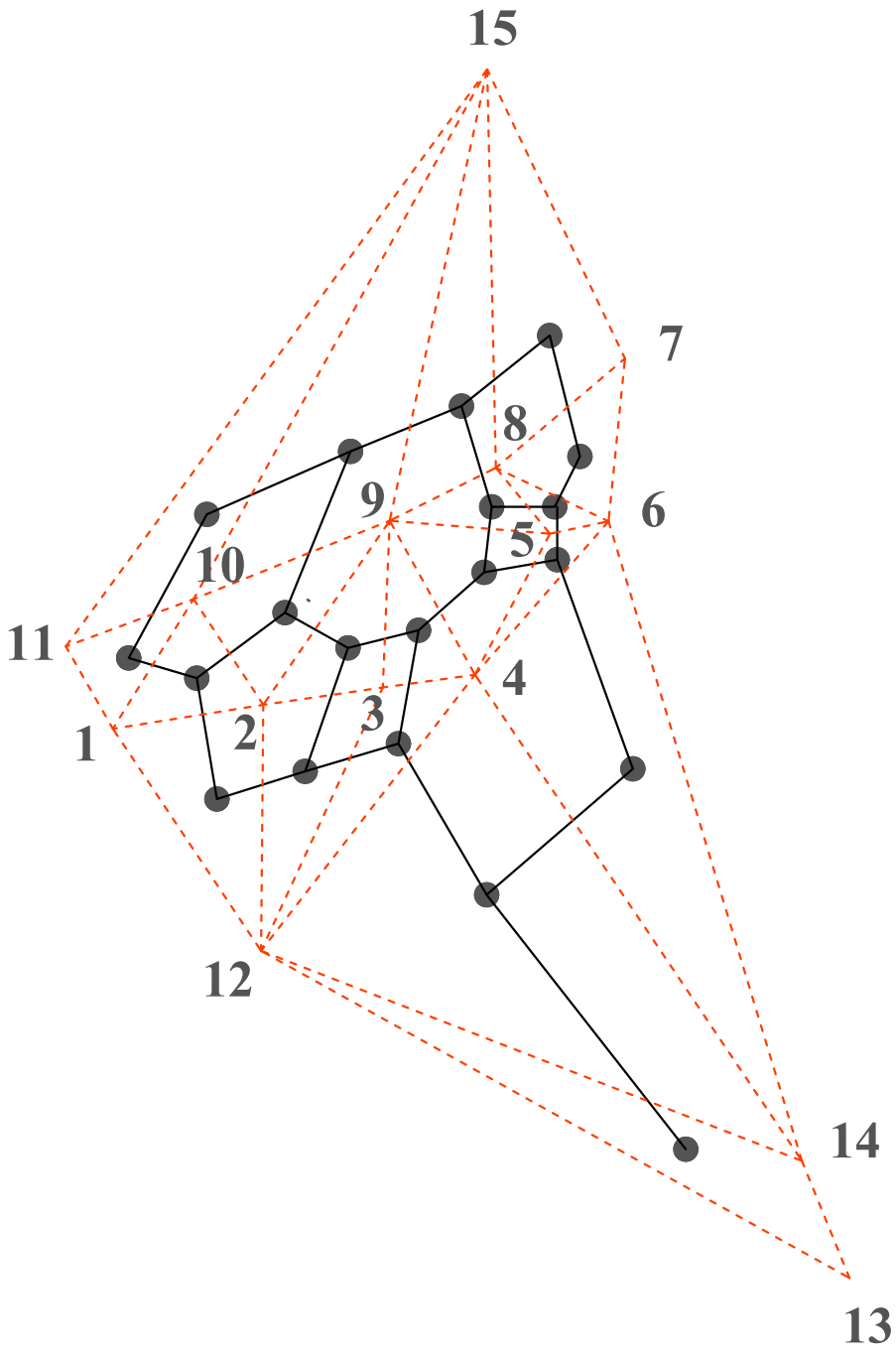

Figure 4: Graph Minor of Delaunay Triangles